HortScience 57(6):698–707. 2022. https://doi.org/10.21273/HORTSCI16510-22

Effects of Different Inorganic Nitrogen Sources of *Iris pseudacorus* and *Iris japonica* on Energy Distribution, Nitrogen, and Phosphorus Removal

Rongrong Duan, Deke Xing, and Tian Chen
Key Laboratory of Modern Agricultural Equipment and Technology of Ministry of Education, School of Agricultural Engineering, Jiangsu University, Zhenjiang 212013, China

Yanyou Wu
State Key Laboratory of Environmental Geochemistry, Institute of Geochemistry, Chinese Academy of Sciences, Guiyang 550081, China

Additional index words. electrophysiological information, cellular metabolic energy, nitrogen metabolism, nitrogen affinity system, phosphorus affinity system

Abstract. **High- and low-affinity transport systems are the main pathways for the transportation of NO_3^- and NH_4^+ across intracellular membranes. NO_3^- and NH_4^+ are assimilated through different metabolic pathways in plants. Fifteen ATP molecules are hydrolyzed in the metabolic process of NO_3^-; however, only five ATP molecules are hydrolyzed in that of NH_4^+. In this research, seedlings of *Iris pseudacorus* and *Iris japonica* were used as the experimental materials in the NO_3^-:NH_4^+ = 30:0, NO_3^-:NH_4^+ = 28:2, NO_3^-:NH_4^+ = 27:3, NO_3^-:NH_4^+ = 15:15, NO_3^-:NH_4^+ = 3:27, and NO_3^-:NH_4^+ = 0:30 treatments at the 7.5 mmol·L^{-1} the total nitrogen content (TN). The intracellular free energy was represented by physiological resistance (R) and physiological impedance (Z) according to the Nernst equation and could conveniently and comprehensively determine the cellular metabolic energy (G_B). The maximum absorption rate (V_{max}) and Michaelis constant (K_m) for NH_4^+ and NO_3^- uptake were calculated according to the kinetic equation. The results showed that the cellular metabolic energy (G_B) of *I. pseudacorus* was 1 to 1.5 times lower than that of *I. japonica* at each treatment on the 10th day. The G_B values of *I. pseudacorus and I. japonica* seedlings increased with increasing NH_4^+ concentration. However, there was a turning point at the NO_3^-:NH_4^+ = 15:15 treatment for the cellular metabolic energy of *I. pseudacorus and I. japonica*. Correlation analysis showed that the value of cellular metabolic energy was negatively correlated with the V_{max} and K_m for NO_3^- uptake, whereas it was positively correlated with that for NH_4^+ uptake. These results demonstrate that the NO_3^-:NH_4^+ = 27:3 treatment level was the most suitable for *I. pseudacorus* and *I. japonica*. This indicates that the greater cellular metabolic energy is the most suitable for plant growth when the concentration of ammonium or nitrate had no significant difference at treatment. These results provide a simple and rapid solution for removal of nitrogen by determination of cellular metabolic energy.**

Nitrate (NO_3^-) and ammonium (NH_4^+) are the primary nitrogen sources for higher plants (Cui et al., 2017; Poothong and Reed, 2016; Tho et al., 2017). High- and low-affinity transport systems (HATS and LATS) are the main pathways for the transportation of nitrate across intracellular membranes (Kochian and Jiao, 1985). The Michaelis constant (K_m) estimated by using the Michaelis equation can be used to determine the pathway of nitrate transport, and a high value of K_m indicates low-affinity NO_3^- uptake. Conversely, a low value of K_m is associated with high-affinity NO_3^- uptake in plants (Kochian and Jiao, 1985; Siddiqi et al., 1992). HATS in plants is activated when the value of K_m is lower than 1 mmol·L^{-1}, whereas LATS is activated when the value of K_m is higher than 1 mmol·L^{-1} (Krapp et al., 2014). The kinetics of NO_3^- absorption are characterized by a linear unsaturated dependence in high-concentration media (Krapp et al., 2014). The transmembrane transport of NH_4^+ can also be conducted through HATS or LATS (Kronzucker et al., 1996). It is dominated by HATS when the concentration of NH_4^+ is lower than 1 mmol·L^{-1}. However, LATS becomes dominant and can be characterized by a linear unsaturated dependence when the concentration of NH_4^+ is ≥1 mmol·L^{-1} (Kronzucker et al., 1996). A high concentration of NH_4^+ will induce HATS and inhibit the activity of ammonium metabolites (Wang et al., 1994).

Phosphorus and phosphorus-containing compounds are not only important constituents of the cytomembrane ATP, nucleic acids, and other living matter but are also necessary participants in the metabolic processes of matter and energy changes; they maintain the normal growth of plants (Hu, 2008). Phosphorus also plays an important role in the utilization of nitrogen by plants. It has been found that the transmembrane transport systems of phosphorus are similar to those of ammonium or nitrate (Hu, 2008). When suffering from phosphorus deficiency, plants absorb phosphorus through HATS, and the unit of K_m is always μmol·L^{-1} (Mei et al., 2012). LATS prevails in plants, and the unit of K_m is mmol·L^{-1} (Muchhal et al., 1996; Nielsen and Barber, 1978). Plants can use alternative transmembrane transport systems to transport ions, and the affinities of those systems are different. As a result, the values of the maximum absorption rate (V_{max}) and K_m will change correspondingly. Research has proven that the removal of ions could be represented by K_m and V_{max} (Chen et al., 2013).

NO_3^- and NH_4^+ are assimilated by different metabolic pathways in plants. Inorganic nitrogen metabolism in plants is shown diagrammatically in Fig. 1 (Liu and Shang, 2016; Wang et al., 2020). Part of NH_4^+ is assimilated to form amino acids and finally synthesizes proteins. Five ATP molecules are hydrolyzed in the metabolic process of NH_4^+. NO_3^- in plants is reduced into NO_2^- by nitrate reductase (NR), and NO_2^- is reduced into NH_3 by nitrite reductase (NIR) when it enters the chloroplast through the plasma membrane. Then the synthesis process of amino acids is similar to that using NH_4^+ (Li et al., 2020; Liu and Shang, 2016; Wang and Lu, 2020). Fifteen ATP molecules are hydrolyzed in the metabolic process of NO_3^-, which means that the assimilation of NO_3^- requires more energy consumption than that of NH_4^+ (Guo et al., 2007). Therefore, we hypothesize that the cellular metabolic energy stored in plants changes when the inorganic nitrogen resources used by plants is altered. The solar energy used by plants is assumed to be Ea, the total energy consumption in the inorganic nitrogen metabolism process is Eb, the cellular metabolic energy stored in plants is G_B, and the energy consumption in other metabolic processes (e.g., EMP, HMP) is Ed (Fig. 1). Here we presume that the values of Ea and Ed are constant, but what if the change trend of G_B as Eb is altered? The accurate determination of G_B is of great importance for the aforementioned investigation.

At present, the cellular metabolic energy in plants is traditionally represented by the

Received for publication 26 Jan. 2022. Accepted for publication 15 Mar. 2022.
Published online 16 May 2022.
This work was funded the Support Plan Projects of Science and Technology Department of Guizhou Province [No. (2021) YB453], the National Natural Science Foundation of China (No. U1612441-2), and Priority Academic Program Development (PAPD) of Jiangsu Higher Education Institutions for supporting this research.
Y.W. and D.X. are the corresponding authors. E-mail: wuyanyou@mail.gyig.ac.cn or xingdeke@ujs.edu.cn.

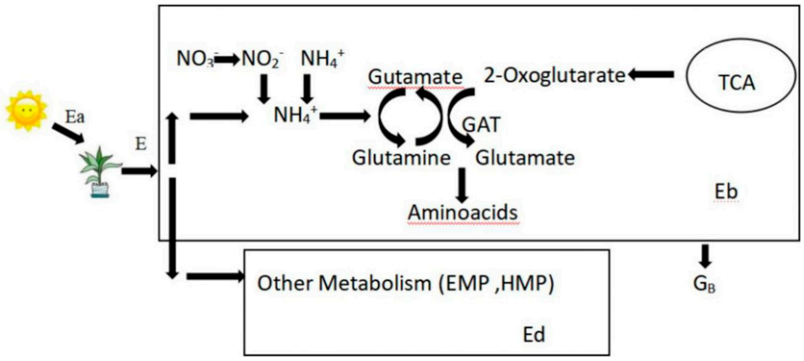

Fig. 1. Relationship between plant metabolism and energy consumption. Ea represents the plant fixed solar energy, E represents the stable chemical energy in plants, Eb represents the total energy consumed by nitrogen metabolism, G_B represents the cellular metabolic energy, and Ed represents the energy consumption by all the other metabolic processes.

intracellular energy state (Hardie and Grahame, 2015). The requirement and supply of metabolic energy in many metabolic processes are still unknown when referring to the assimilation and alienation of matter. Therefore, the cellular metabolic energy cannot simply be determined by the intracellular energy and charge state (Reuveni, 1992). In this research, the electrical energy is coupled with the resistance (R), impedance (Z), and capacitor (C) according to the Nernst equation, and the intracellular free energy is represented by R and Z to conveniently and comprehensively determine the cellular metabolic energy (Mwesigwa et al., 2000). The mesophyll cell can be regarded as a concentric sphere capacitor with both inductor and resistor functions. The resistive current is produced when the ion is transported across the cell membrane and is affected by the permeability of the cell membrane and the quantity of permeable ions (Mark et al., 2008; Stitt, 1999). The cell membrane permeability is influenced by the external stimulus, which changes the ion concentrations inside and outside the membrane. The Nernst equation can be applied to the difference in the ion concentrations mentioned earlier (Aoki, 1991; Schönleber and Ivers-Tiffée, 2015). Physiological resistance is inversely proportional to EC, and EC is proportional to the ion concentration in cells. As such, the relationship between physiological R or Z and external stimuli can be derived. Cellular metabolic energy can be more conveniently and comprehensively determined, in a more timely manner, by electrophysiological parameters than by the measurement of intracellular energy and charge state (Anderson, 1980; Ramage, 2002).

Iris pseudacorus and *Iris japonica* are both fast-growing plants with a strong ability to remove inorganic nitrogen (Chen et al., 2013). *I. pseudacorus* is a typical plant growing in aquatic and terrestrial environments. Studies have shown that *I. pseudacorus* grows better than *I. japonica* in the polluted water (Abe et al., 1991). Currently, most studies focus on the nitrogen absorption and efficiency of the aforementioned plants in water, and the absorption kinetics of NH_4^+, NO_3^-, and $H_2PO_4^-$ are also hot topics (Zhu et al., 2020). It has been found that *I. pseudacorus* had significant advantages in removing high concentration of nitrogen and phosphorus (NH_4^+: 180–220 mg·L^{-1}, TP: 30–35 mg·L^{-1}) (Feng et al., 2020). Researchers have also reported that the total nitrogen and phosphorus removal rate of *I. pseudacorus* were 48.84% and 46.13%, and *I. pseudacorus* has a strong ability to remove nitrogen and phosphorus (Ji et al., 2015; Yang et al., 2017). However, there is little research on the total nitrogen and phosphorus removal of *I. japonica*. In this research, seedlings of *I. pseudocorus* and *I. japonica* were used as the experimental materials, the variation of energy distribution in the two plant species and the removal of nitrogen or phosphorus in water were investigated under different inorganic nitrogen resources, and the relationship between energy distribution and removal of nitrogen or phosphorus was analyzed. This study provides a theoretical basis for improving the removal efficiency of different proportions of nitrogen in water and maintaining ecological balance.

Materials and Methods

Experimental materials. Seedlings (20–30 cm) of *I. pseudacorus* and *I. japonica* were obtained from an online shopping platform in China. They were cultivated in half-strength Hoagland solution for one month before applying inorganic nitrogen treatment.

Experimental design. The experiment was carried out at the Institute of Agricultural Engineering, Jiangsu University, Jiangsu Province, China. The seedlings of *I. pseudacorus* and *I. japonica* were cultivated in water under a 12 h photoperiod (260 ± 20 μmol·m^{-2}·s^{-1}), day/night temperature cycle of 28–30°C and relative humidity of 65% ± 5%. The concentrations of dissolved O_2 were constantly supplied and were no less than 0.625 mmol·L^{-1}. The water environment for the treatment was artificially simulated by using Hoagland solution. Each tray contained 10 L modified Hoagland's solution, and water was added into the tray every day to maintain the content of the solution.

Taking the concentration of the urban pollutant emission standard (GB18918-2002) and the environmental quality standard of the surface water (GB3838-2002) as references, the total nitrogen content (TN) of Hoagland's solution was calculated to be 7.5 mmol·L^{-1}. Six NO_3^-/NH_4^+ proportions (30:0, 28:2, 27:3, 15:15, 3:27, and 0:30) (Table 1) were prepared by adding KNO_3, $Ca(NO_3)_2$, NH_4NO_3 and $(NH_4)_2SO_4$ into Hoagland's solution. The seedlings of *I. pseudacorus* were subjected to these six levels of treatment and marked as ps-1 (30:0), ps-2 (28:2), ps-3 (27:3), ps-4 (15:15), ps-5 (3:27), and ps-6 (0:30). The seedlings of *I. japonica* were simultaneously subjected to these six levels of treatment and marked as ja-1 (30:0), ja-2 (28:2), ja-3 (27:3), ja-4 (15:15), ja-5 (3:27), and ja-6 (0:30). The seedlings of *I. pseudacorus* and *I. japonica* before the treatment are marked as ps-0 and ja-0, respectively. To prevent the conversion of ammonium to nitrate nitrogen, 0.0035 mmol·L^{-1} nitrification inhibitor dicyandiamide ($C_2H_4N_4$) was added to the treatment solution at each level. The treatment lasted for 10 d.

Determination of physiological capacitance, resistance, and impedance. The third youngest fully expanded leaves from the top (five plants from each treatment group) were chosen for measurements. The leaves were soaked in water for 30 min to ensure that they were saturated. The leaf surface was then immediately sucked up, and the measurement site (10 cm away from the top) on the leaves was marked. The leaf was clamped at the parallel electrode plates of the measurement device, and the clamping force was changed by changing the number of weights (100 g per weight). The physiological C, R, and Z were measured using an LCR tester (Model 3532-50; Hioki, Nagano, Japan), and the frequency and voltage were set as 3 kHz and 1 V, respectively (Fig. 2).

Calculation of leaf cellular metabolic energy based on physiological capacitance, resistance, and impedance. The mesophyll cells can be regarded as concentric sphere capacitors with both inductor and resistor functions. The leaf was clamped between the two parallel plates of the capacitor to form a parallel plate capacitor. The elasticity and plasticity of the mesophyll cells was changed, further leading to a change in the dielectric constant of the solute in leaf tissue. The physiological capacitance was affected.

The gravity equation is:

$$F = (M_0 + m)g, \quad [1]$$

where F is gripping force (N), M is the mass of weights (kg), m is the mass of plastic rod and electrode (kg), and g is the gravitational acceleration with a value of 9.8.

Table 1. The concentration of NO_3^-, NH_4^+, and total nitrogen.

NO_3^-/NH_4^+	TN (mmol·L^{-1})	C_{NO3^-} (mmol·L^{-1})	C_{NH4^+} (mmol·L^{-1})
30:02 (ps-1 or ja-1)	7.50	7.50	0.00
28:2 (ps-2 or ja-1)	7.50	7.00	0.50
27:3 (ps-3 or ja-3)	7.50	6.75	0.75
15:15 (ps-4 or ja-4)	7.50	3.75	3.75
3:27 (ps-5 or ja-5)	7.50	0.75	6.75
0:30 (ps-6 or ja-6)	7.50	0.00	7.50

ps = the growth indices of *I. pseudacorus*; ja = the growth indices of *I. japonica*.

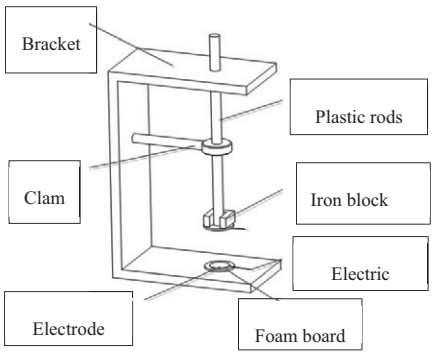

Fig. 2. The parallel-plate capacitor.

The Gibbs's free energy equation is:

$$\Delta G = \Delta H + PV. \quad [2]$$

The equation for the energy of the capacitor is:

$$W = \frac{1}{2}U^2C. \quad [3]$$

ΔH is the internal energy of the system (plant leaf system composed of cells), P is the pressure imposed on plant cells, V is the volume of plant cells, U is the test voltage, and C is the physiological capacitance of plant leaves.

P can be calculated as follows:

$$P = \frac{F}{S}. \quad [4]$$

where F is the clamping force and S is the effective area of the leaf in contact with the action capacitor plates.

According to the energy conservation law, a capacitor's energy is equal to the work converted by Gibbs's free energy, i.e., W = ΔG. The physiological capacitance (C) is expressed using Eq. [5]:

$$C = \frac{2\Delta H}{U^2} + \frac{2V}{SU^2}F. \quad [5]$$

Assuming d represents the specific effective thickness of plant leaves, that is $d=\frac{V}{S}$; Eq. [5] is then rewritten as:

$$C = \frac{2\Delta H}{U^2} + \frac{2d}{U^2}F. \quad [6]$$

Incorporating $x_0 = \frac{2\Delta H}{U^2}$, $h = \frac{2d}{U^2}$ into Eq. [6], it is then changed to be:

$$C = x_0 + hF, \quad [7]$$

where x_0 and h are model parameters.

The d is then calculated as follows:

$$d = \frac{U^2h}{2}. \quad [8]$$

The Nernst equation is:

$$E - E_0 = \frac{RT}{nF_0}\ln\frac{C_i}{C_0}, \quad [9]$$

where E is the electromotive force (V), E_0 is the standard electromotive force (V), R is the gas constant (8.31 J·K^{-1}·mol^{-1}), T is the thermodynamic temperature (K), C_i is the intracellular ion concentration (mol·L^{-1}), C_0 is the extracellular ion concentration (mol·L^{-1}), F_0 is the Faraday constant (9.65 × 10^4 C·mol^{-1}), and n is the ion transfer amount (mol).

In mesophyll cells, vacuoles and cytoplasm occupy most of the space in the cell. The sum of C_0 and C_i is certain for mesophyll cell. It is equal to the total amount of permeable ions (C_T) inside and outside the membrane in response to physiological resistance, and C_i is directly proportional to the EC. The conductivity is the reciprocal of resistance (R).

The $\frac{C_i}{C_0}$ is expressed as follows:

$$\frac{C_i}{C_0} = \frac{\frac{f_0}{R}}{C_T - \frac{f_0}{R}} = \frac{f_0}{C_TR - f_0}. \quad [10]$$

The internal energy of the electromotive force (E) can be transformed into work produced by the pressure PV = aE.

$$PV = aE = aE_0 + \frac{aRT}{nF_0}\ln\frac{C_i}{C_0}, \quad [11]$$

where P is the pressure imposed on plant cells; a is the transfer coefficient from electromotive force to energy; and V is the volume of plant cells. Eq. [10] into Eq. [11], and Eq. [12] are then rewritten as follows:

$$PV = aE = aE_0 - \frac{aRT}{nR}\ln\frac{C_TR - f_0}{f_0}. \quad [12]$$

Then:

$$\ln\frac{C_TR}{f_0} = \frac{nF_0E_0}{RT} - \frac{VnF_0}{SART}F. \quad [13]$$

The logarithmic Eq. [13] written in base e can be solved as follows:

$$\frac{C_TR - f_0}{f_0} = e^{\frac{nF_0E_0}{RT}}e^{\frac{-VnF_0F}{SaRT}}. \quad [14]$$

The resistance can be calculated as follows:

$$R = \frac{f_0}{C_T} + \frac{f_0}{C_T}e^{\frac{nF_0E_0}{RT}}e^{\frac{-dnFF_0}{aRT}}. \quad [15]$$

Incorporating $y = \frac{f_0}{C_T}$, $k_1 = \frac{f_0}{C_T}e^{\frac{nF_0E_0}{RT}}$, $b_1 = \frac{dnF_0}{RTa}$ into Eq. [15], it is then rewritten as:

$$R = y_0 + k_1e^{-b_1F}. \quad [16]$$

where y_0, k_1, and b_1 are the parameters.

The equation of unit cellular metabolic energy based on physiological resistance is:

$$\Delta G_{R-E} = \frac{aE_0}{d} = \frac{\ln k_1 - \ln y_0}{b_1}. \quad [17]$$

Then,

$$\Delta G_R = \Delta G_{R-E} \times d. \quad [18]$$

Similarly,

$$E - E_0 = \frac{R_0T}{n_ZF_0}\ln\frac{Q_i}{Q_0}. \quad [19]$$

The physiological resistance (Z) of plant leaves with increasing clamping force is expressed as follows:

$$Z = p_0 + k_2e^{-Fb_2}, \quad [20]$$

where p_0, k_2, and b_2 are the parameters.

Therefore, the unit cellular metabolic energy of leaf cells based on physiological impedance is:

$$\Delta G_{Z-E} = a\frac{E_0}{d} = \frac{\ln k_2 - \ln p_0}{b_2}. \quad [21]$$

The metabolic energy of plant leaves based on physiological impedance is:

$$\Delta G_Z = \Delta G_{Z-E} \times d. \quad [22]$$

The equation of cellular metabolic energy (G_B) is as follows:

$$G_B = \frac{\Delta G_Z + \Delta G_R}{2}. \quad [23]$$

Determination of nitrogen and phosphorus contents. The water samples (20 mL) at each treatment level were measured on the 10th day. The concentrations of NH_4^+, NO_3^- and PO_4^- in water were determined by the following methods: NH_4^+-Nessler colorimetric spectrophotometer (Tan and Mao, 1998); NO_3^--Thymol spectrophotometry (Sun et al., 2007); PO_4^--ammonium molybdate spectrophotometer (Wei, 2003).

Calculation of kinetic parameters. The contents of NO_3^-, NH_4^+, and PO_4^- in the samples were calculated according to the standard curve.

The equation is:

$$p_{N-N_0} = \frac{m}{V}, \quad [24]$$

where $p_{(N-N0)}$ is the nitrogen content in the water sample (mg·L^{-1}), m is the value of the nitrogen content calculated according to the standard curve, and v is the volume of the measured water sample (mL).

The kinetic equation is then expressed as follows:

$$\Delta V = \frac{V_{max}C}{K_m + C}, \quad [25]$$

where V is the absorption rate (mmol·L^{-1}·H^{-1}), V_{max} is the maximum absorption rate (mmol·L^{-1}·H^{-1}), C is the ion concentration in the external solution (mmol·L^{-1}), and K_m is the Michaelis constant (mmol·L^{-1}).

The correlation between the ion concentration and the absorption time is expressed

as follows:

$$Y = c + bX + aX^2, \quad [26]$$

where Y is the ion concentration; X is the absorption time; and a, b, and c are the fitting parameters.

The derivative of Eq. [25] is as follows:

$$Y = -bX - aX^2. \quad [27]$$

The V_{max} is expressed as follows (where N is absorbed liquid volume):

$$V_{max} = -b \times N. \quad [28]$$

Incorporating $Y = \frac{V_{max}}{2}$ into Eq. [26], the X value in the equation seems to be the K_m value.

Measurement of growth index. The heights of plants (three plants from each treatment group) were determined by a ruler. The fresh weights of roots and leaves (three plants from each treatment group) were determined on the 10th day. The dry weights of leaves and roots (three plants from each treatment group) were measured after deactivation at 150 °C and drying blade at 60–70°.

Measurement of photosynthetic parameters. The second fully expanded leaves were selected for the gas exchange measurement from 9:00 AM to 11:30 AM on sunny days. A portable LI-6400XT photosynthetic measurement system was used to determine the net photosynthesis rate (P_N, μmol·m^{-2}·s^{-1}).

Statistical analysis. Excel and Origin software were used to analyze the experimental data. Data were analyzed using exploratory data analysis by SPSS software (version 15.0, SPSS Inc.). A correlation matrix was generated by Pearson's correlation coefficients.

Results

Fitting curves of the relationship between C, R, Z, and F. The linear relationships between C and F of *I. pseudacorus* (Fig. 3A) and *I. japonica* (Supplemental Fig. 1) were fitted using Sigmaplot software. Linear curves of the relationship between the C and F of *I. pseudacorus* (Fig. 3A) and *I. japonica* (Supplemental Fig. 1A) were fitted through Sigmaplot software. However, the values of R and Z in *I. pseudacorus* (Fig. 3B and C) and *I. japonica* (Supplemental Fig. 1B and C) logarithmically decreased as the values of F increased.

Cellular metabolic energy under different inorganic nitrogen sources. The values of cellular metabolic energy (G_B) of *I. pseudacorus* and *I. japonica* were calculated according to Eq. [23]. As shown in Fig. 4A and B, the G_B value of *I. japonica* at ja-0 was higher than that of *I. pseudacorus* at ps-0. The G_B of *I. japonica* became 1 to 1.5 times higher than that of *I. pseudacorus* at each treatment level on the 10th day. The G_B values of *I. pseudacorus and I. japonica* increased as the NH_4^+ concentration increased. However, a significant difference between the values of G_B in *I. pseudacorus* at ps-4 and those in *I. japonica* at ja-4 was observed.

There was no significant difference between the values of G_B in *I. pseudacorus* at ps-0 and ps-2 (Fig. 4A). The G_B value of *I. pseudacorus* at the ps-1 level was the lowest and that at the ps-6 level was the highest (Fig. 4A). The G_B values of *I. pseudacorus* clearly increased at the ps-3 and ps-4 levels compared with the ps-2 or ps-1 level. However, the G_B values of *I. pseudacorus* at the ps-3 and ps-4 levels showed no significant difference. The G_B value

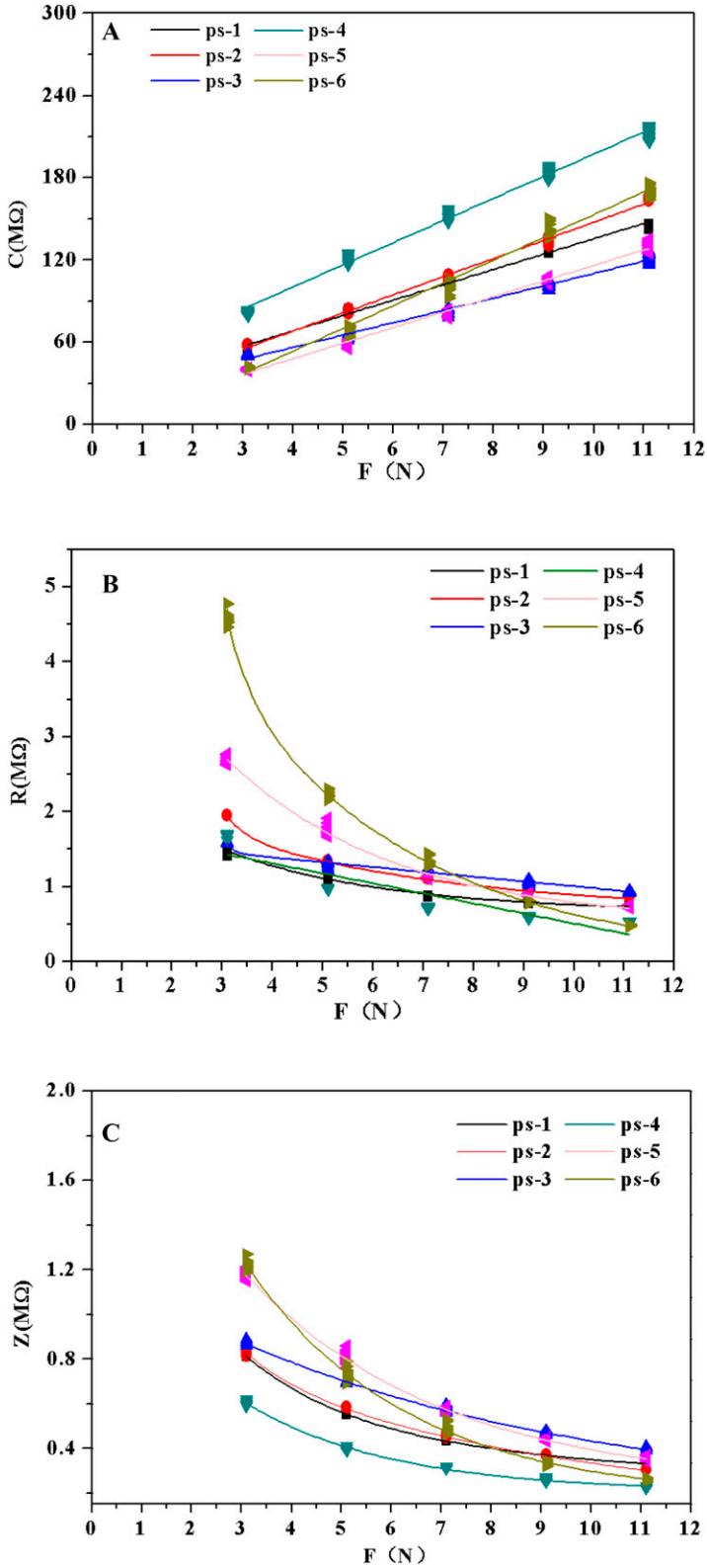

Fig. 3. Fitting curves of the relationships among capacitance (C), resistance (R), impedance (Z), and gripping force (F) of *I. pseudacorus* under different inorganic nitrogen sources. (**A**) The relationship between the physiological C and F of *I. pseudacorus*. (**B**) The relationship between the physiological R and F of *I. pseudacorus*. (**C**) The relationship between the physiological Z and F of *I. pseudacorus*.

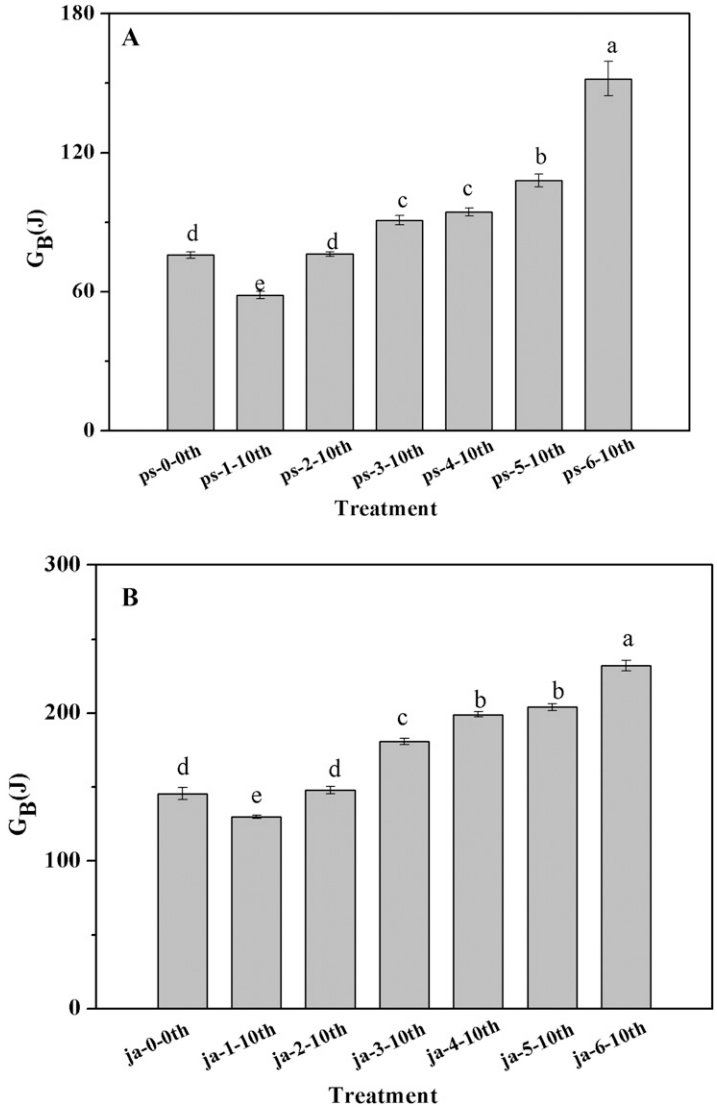

Fig. 4. Effects of different inorganic nitrogen sources on the cellular metabolic energy of *I. pseudacorus* and *I. japonica* on the 10th day. ps-0 and ja-0 are the cellular metabolic energies of *I. pseudacorus* and *I. japonica* before the treatment, respectively. The cellular metabolic energy of (**A**) *I. pseudacorus* and (**B**) *I. japonica* on the 10th day. Different letters appear above the error bars when subsequent values differ significantly at the 5% level ($P < 0.05$).

of *I. pseudacorus* at ps-5 was lower than that at ps-6 but higher than that at the ps-3 and ps-4 levels.

There was no significant difference between the G_B values of *I. japonica* at the ja-0 and ja-2 levels (Fig. 4B). The G_B value of *I. japonica* at the ja-1 level was ≈120 J, which was the lowest, and the highest G_B value of *I. japonica* was observed at the ja-6 level. The G_B values of *I. japonica* increased with increasing ammonium nitrogen between the levels ranging from ja-1 to ja-6 (Fig. 4B). However, the G_B values of *I. japonica* at the ja-4 and ja-5 levels exhibited no significant difference on the 10th day.

Effects of different nitrogen sources on growth indices. The leaf fresh weights of *I. pseudacorus* at the ps-3 and ps-2 levels were significantly higher than other levels on the 10th day (Table 2). The leaf fresh weights of *I. pseudacorus* at the ps-0, ps-4, ps-5, and ps-6 levels showed no significant difference but were clearly lower than those at the ps-1, ps-2, and ps-3 levels on the 10th day. The root fresh weight of *I. pseudacorus* on the 10th day increased significantly compared with the ps-0 level, but there was no significant difference between the levels ranging from ps-1 to ps-6. The highest values of leaf and root dry weight of *I. pseudacorus* were all observed at the ps-2 and ps-3 levels. The values of leaf dry weight and root dry weight showed no significant difference between the levels ranging from ps-4 to ps-6. The lowest value of height of *I. pseudacorus* was observed at the ps-0 level, and the highest value appeared at the ps-2 and ps-3 levels. The height of *I. pseudacorus* increased between the levels ranging from ps-0 to ps-3 but decreased between the levels ranging from ps-3 to ps-6.

There was no significant difference between the values of the leaf fresh and dry weight of *I. japonica* at ja-1, ja-2, and ja-3 (Table 2). However, these values were higher than those at other levels, and the lowest values of leaf fresh and dry weight were all observed at the ja-0 level. A higher value of root fresh and dry weight of *I. japonica* was associated with increasing ammonium concentration between the levels ranging from ja-1 to ja-3. The root fresh and dry weight of *I. japonica* decreased between the levels ranging from ja-4 to ja-6. Higher values of plant height of *I. japonica* were associated with increasing ammonium concentration between the levels ranging from ja-1 to ja-3. The values of plant height at the ja-4, ja-5, and ja-6 levels showed no significant difference.

Kinetic parameters for NH_4^+, NO_3^-, and PO_4^- uptake in I. pseudacorus. Fitting curves of the relationship between ion concentration and absorption time (h) in *I. pseudacorus* are shown in Fig. 5. The correlation coefficients (R^2) of the fitting equations for *I. pseudacorus* were 0.93 to 0.99. The kinetic parameters K_m and V_{max} for NH_4^+, NO_3^-, and PO_4^- uptake were calculated according to Eq. [25] and are shown in Table 3.

As shown in Table 3, the K_m for NO_3^- uptake in *I. pseudacorus* at the ps-1 and ps-2 levels was significantly higher than that at the ps-3, ps-4, and ps-5 levels and the lowest K_m for NO_3^- uptake in *I. pseudacorus* at the ps-5 level. The K_m for NO_3^- uptake in *I. pseudacorus* exhibited no significant differences at the ps-1 and ps-2 and the ps-3 and ps-4 levels. The value of V_{max} for NO_3^- uptake in *I. pseudacorus* at ps-1 was the highest and then decreased with increasing ammonium concentration between the levels ranging from ps-1 to ps-5.

The V_{max} for NH_4^+ uptake in *I. pseudacorus* at the ps-2 level was the lowest and then increased with increasing ammonium concentration between the levels ranging from ps-2 to ps-6 (Table 3). The K_m for NH_4^+ uptake in *I. pseudacorus* at the ps-6 level was the highest. The K_m for NH_4^+ uptake in *I. pseudacorus* at the ps-4 level was significantly higher than those at the ps-3 and ps-2 levels. However, the K_m for NH_4^+ uptake in *I. pseudacorus* at the ps-2 level exhibited no significant differences from that at the ps-3 level.

The higher values of V_{max} for PO_4^- uptake in *I. pseudacorus* at the ps-3, ps-4, and ps-5 levels compared with those at the ps-1, ps-2, and ps-6 levels are shown in Table 3. There was no significant difference between the values of V_{max} for PO_4^- uptake in *I. pseudacorus* at levels ranging from ps-3 to ps-5. The value of V_{max} for PO_4^- uptake in *I. pseudacorus* at the ps-2 level was clearly lower than those at the ps-3, ps-4, and ps-5 levels. The values of V_{max} for PO_4^- uptake in *I. pseudacorus* at the ps-1 and ps-6 levels were lowest. The values of V_{max} for PO_4^- uptake in *I. pseudacorus* was no significant difference between the values at the ps-1 and ps-6 levels. The values of K_m for PO_4^- uptake in *I. pseudacorus* at the ps-3 and ps-6 levels were lower than those at other levels, and there was no significant difference between the values at these levels (ps-1, ps-2, ps-4, and ps-5).

Table 2. Effects of different inorganic nitrogen sources on the growth indices of *I. pseudacorus* and *I. japonica*.

Number	Fresh leaf wt (g)	Fresh root wt (g)	Dry leaf wt (g)	Dry root wt (g)	Ht (cm)
ps-0 d[z]	7.86 ± 0.12 c	3.60 ± 0.11 b	0.88 ± 0.02 c	0.62 ± 0.02 b	53.43 ± 1.12 f
ps-1-10 d	14.05 ± 0.94 b	3.93 ± 0.11 a	1.57 ± 0.11 b	0.68 ± 0.00 b	69.96 ± 0.37 c
ps-2-10 d	18.15 ± 0.90 a	4.02 ± 0.06 a	2.10 ± 0.03 a	1.02 ± 0.04 a	72.86 ± 0.87 b
ps-3-10 d	18.25 ± 0.34 a	4.19 ± 0.05 a	2.24 ± 0.08 a	1.25 ± 0.05 a	75.68 ± 1.10 a
ps-4-10 d	8.51 ± 0.11 c	3.96 ± 0.05 a	1.01 ± 0.04 c	0.67 ± 0.02 b	65.85 ± 0.34 d
ps-5-10 d	7.64 ± 0.12 c	3.84 ± 0.13 a	0.88 ± 0.06 c	0.68 ± 0.01 b	64.11 ± 1.46 d
ps-6-10 d	7.66 ± 0.03 c	3.87 ± 0.12 a	0.90 ± 0.08 c	0.65 ± 0.02 b	63.03 ± 0.30 e
ja-1-0 d[y]	3.94 ± 0.12 f	0.73 ± 0.03 f	1.06 ± 0.04 d	0.22 ± 0.01 f	19.98 ± 1.11 e
ja-1-10 d	6.45 ± 0.14 a	1.65 ± 0.05 b	1.94 ± 0.04 a	0.49 ± 0.01 b	27.50 ± 0.62 c
ja-2-10 d	7.02 ± 0.06 a	1.78 ± 0.04 ab	2.11 ± 0.02 a	0.54 ± 0.01 ab	30.17 ± 0.37 b
ja-3-10 d	7.09 ± 0.08 a	1.84 ± 0.04 a	2.13 ± 0.03 a	0.55 ± 0.01 a	34.17 ± 0.85 a
ja-4-10 d	4.39 ± 0.26 c	0.55 ± 0.05 c	1.32 ± 0.08 c	0.17 ± 0.01 c	23.73 ± 0.75 d
ja-5-10 d	5.18 ± 0.15 b	1.41 ± 0.03 d	1.55 ± 0.04 b	0.42 ± 0.01 d	25.72 ± 0.58 cd
ja-6-10 d	4.88 ± 0.34 bc	1.07 ± 0.06 e	1.47 ± 0.10 bc	0.32 ± 0.02 e	23.51 ± 1.15 d

[z]ps-0 = the growth indices of *I. pseudacorus* before the treatments.

[y]ja-0 = the growth indices of *I. japonica* before the treatments.

ps = the growth indices of *I. pseudacorus*; ja = the growth indices of *I. japonica*.

The 10 d in the first column indicates the 10th day.

The mean ± SE is followed by different lowercase letters in the same column when values differ significantly at $P \leq 0.05$ according to one-way ANOVA.

Kinetic parameters for NH_4^+, NO_3^-, and PO_4^- uptake in I. japonica. Lower values of V_{max} for NO_3^- uptake in *I. japonica* were associated with different inorganic nitrogen sources between the levels ranging from ja-1 to ja-5 (Table 4). However, the values of V_{max} for NO_3^- uptake in *I. japonica* at the ja-2 and ja-3 levels showed no significant differences. The value of K_m for NO_3^- uptake in *I. japonica* clearly decreased as inorganic nitrogen sources changed from ja-1 to ja-5.

The value of V_{max} for NH_4^+ uptake in *I. japonica* at the ja-2 level was the lowest and that at the ja-6 level was the highest (Table 4). The values of V_{max} for NH_4^+ uptake (*I. japonica*) at the ja-4 and ja-5 levels were lower than those at ja-6 and showed no significant difference at the ja-4 and ja-5 levels, whereas the V_{max} for NH_4^+ uptake in *I. japonica* at the ja-3 level remained relatively low. The K_m values for NH_4^+ uptake in *I. japonica* at the ja-6 level were the highest, and the values increased with increasing NH_4^+ concentration between the levels ranging from ja-2 to ja-6.

The lowest value of V_{max} for PO_4^- uptake in *I. japonica* was observed at the ja-1 and ja-4 levels (Table 4). The value of V_{max} for PO_4^- uptake (*I. japonica*) at the ja-2 level showed no significant difference from those at the ja-5 and ja-6 levels but was clearly lower than that at the ja-3 level. The K_m for PO_4^- uptake in *I. japonica* at the ja-1 level was the lowest and increased with increasing ammonium nitrogen between the levels ranging from ja-4 to ja-6. However, the values of K_m for PO_4^- uptake (*I. japonica*) at the ja-2, ja-3, and ja-4 levels exhibited no significant difference.

Correlation of parameters. The Pearson correlation coefficients for the relationship of ps-G_B, V_{max}, and K_m for NH_4^+, NO_3^-, and PO_4^- uptake in *I. pseudacorus* are shown in Table 5. ps-G_B had a significant positive correlation with PO_4^--K_m, NH_4^+-V_{max}, and NH_4^+-K_m and a significant negative correlation with NO_3^--V_{max} and NO_3^--K_m. However, ps-G_B exhibited no significant correlation with PO_4^--V_{max}. PO_4^--K_m was significantly correlated with NH_4^+-V_{max}, NH_4^+-K_m, NO_3^--V_{max}, and NO_3^--K_m. PO_4^--V_{max} exhibited no significant correlation with NH_4^+-V_{max}, NH_4^+-K_m, NO_3^--V_{max}, and NO_3^--K_m.

Table 6 shows that there was a good correlation between ja-G_B and the kinetic parameters for NH_4^+, NO_3^-, and PO_4^- uptake in *I. japonica*, that is, V_{max} and K_m. ja-G_B had a significant positive correlation with PO_4^--K_m, NH_4^+-V_{max}, and NH_4^+-K_m and a significant negative correlation with NO_3^--V_{max} and NO_3^--K_m. However, ja-G_B exhibited no significant correlation with PO_4^--V_{max}. PO_4^--K_m was significantly correlated with NH_4^+-V_{max}, NH_4^+-K_m, NO_3^--V_{max}, and NO_3^--K_m. PO_4^--V_{max} exhibited no significant correlation with NH_4^+-V_{max}, NH_4^+-K_m, NO_3^--V_{max}, and NO_3^--K_m.

Net photosynthetic rate under different inorganic nitrogen sources. As shown in Fig. 6A and B, the P_N of *I. pseudacorus* was higher than that of *I. japonica* at same treatment level. However, the P_N of *I. pseudacorus* at the ja-0, ja-1, and ja-2 levels showed no significant differences. The P_N of *I. pseudacorus* at the ps-3 higher than those at other treatments. The P_N of *I. pseudacorus* at ps-4 to ps-6 were lowest those at the ps-3.

The P_N of *I. japonica* at the ps-3 higher than that of other treatments. The P_N of *I. japonica* from ja-4 to ja-6 was lower than the ja-0, ja-1, ja-2, and ja-3. However, the P_N of *I. japonica* at the ja-0, ja-1, and ja-2 levels showed no significant differences.

Discussion

The assimilation and catabolism processes include hydrogen exchange, assimilation, and utilization of inorganic matter, synthesis, and transformation of organic matter and energy, physiological processes, and other biochemical processes (Shu et al., 2016). The activities of those processes can be directly reflected by the cellular metabolic energy in plants (Vanhercke et al., 2014). First, in this study, the cellular metabolic energy stored in *I. pseudacorus* and *I. japonica* plants both increased with increasing ammonium concentration (Fig. 4). Nitrogen metabolism, which is an important part of assimilation and catabolism in plants, is closely related to metabolic energy (Wang and Lu, 2020). Compared with the nitrogen metabolism of NH_4 , that of NO_3^- requires more energy in the processes of nitrogen metabolism (Guo et al., 2007; Konnerup et al., 2010). The cellular metabolic energy stored in plants is affected by the energy consumption of the nitrogen metabolism of NH_4^+ and NO_3^-. When the concentration of the total nitrogen is same, the increase of NH_4^+ concentration can increase the cellular metabolic energy stored in *I. pseudacorus* and *I. japonica*. Second, the cellular metabolic energy stored in *I. pseudacorus* plants at each level was lower than that of *I. japonica* (Fig. 4). It indicated that the purification rate of *I. japonica* was relatively lower compared with *I. pseudacorus* (Yuan et al., 2018). In other words, *I. pseudacorus* and *I. japonica* showed different demands for nitrogen during growth and development (Colmer and Bloom, 1998). The removal of ions could be represented by K_m and V_{max} (Zhu et al., 2020). A low value of K_m and a high value of V_{max} indicate a high removal efficiency of ions from wastewater (Zhu et al., 2020). The results shown that the V_{max} for NO_3^- and NH_4^+ uptake by *I. pseudacorus* was 1.5 to 2 times higher than that by *I. japonica* (Tables 3 and 4), which demonstrated that the removal of NO_3^- and NH_4^+ by *I. pseudacorus* was higher than that by *I. japonica*. Correlation analysis showed that the cellular metabolic energy stored in plants was correlated with the kinetic parameters of NO_3^- and NH_4^+ absorption (Tables 5 and 6). The results inferred that the strong removal of NO_3^- and NH_4^+ had consumed more energy for nitrogen metabolism. The cellular metabolic energy stored in the *I. pseudacorus* had reduced.

Third, there was a turning point at the ps-3 and ps-4 levels for the cellular metabolic energy of *I. pseudacorus* (Fig. 4A). However, that of *I. japonica* was observed at the ja-4 and ja-5 levels (Fig. 4B). The reasons for this phenomenon were as follows: first, the cellular metabolic energy could affect the phosphate (Guo et al., 2006). The phosphorus increased the activities of NR and glutamine systhetase (GS) in Flag leaves of wheat (Wang et al., 2006). During the nitrogen metabolism, some key enzymes, e.g., NR and GS, participate in these processes (Xu and Zhou, 2004). The results showed that the cellular metabolic energy of *I. japonica and I. pseudacorus* was positively correlated with the K_m values for PO_4^- uptake (Tables 5 and 6). The K_m values for PO_4^- uptake in *I. pseudacorus* at the ps-4 level was significantly higher than that at the ps-3 treatment, which indicated that the phosphorus in *I. pseudacorus* at the ps-4 level was lower than that at the ps-3 treatment level. Phosphorus deficiency could decrease the activities of GS in *I. pseudacorus* at the ps-4 level. The activities of NR and GS could affect the assimilation process of NO_3^- and NH_4^+ (Xu and Zhou,

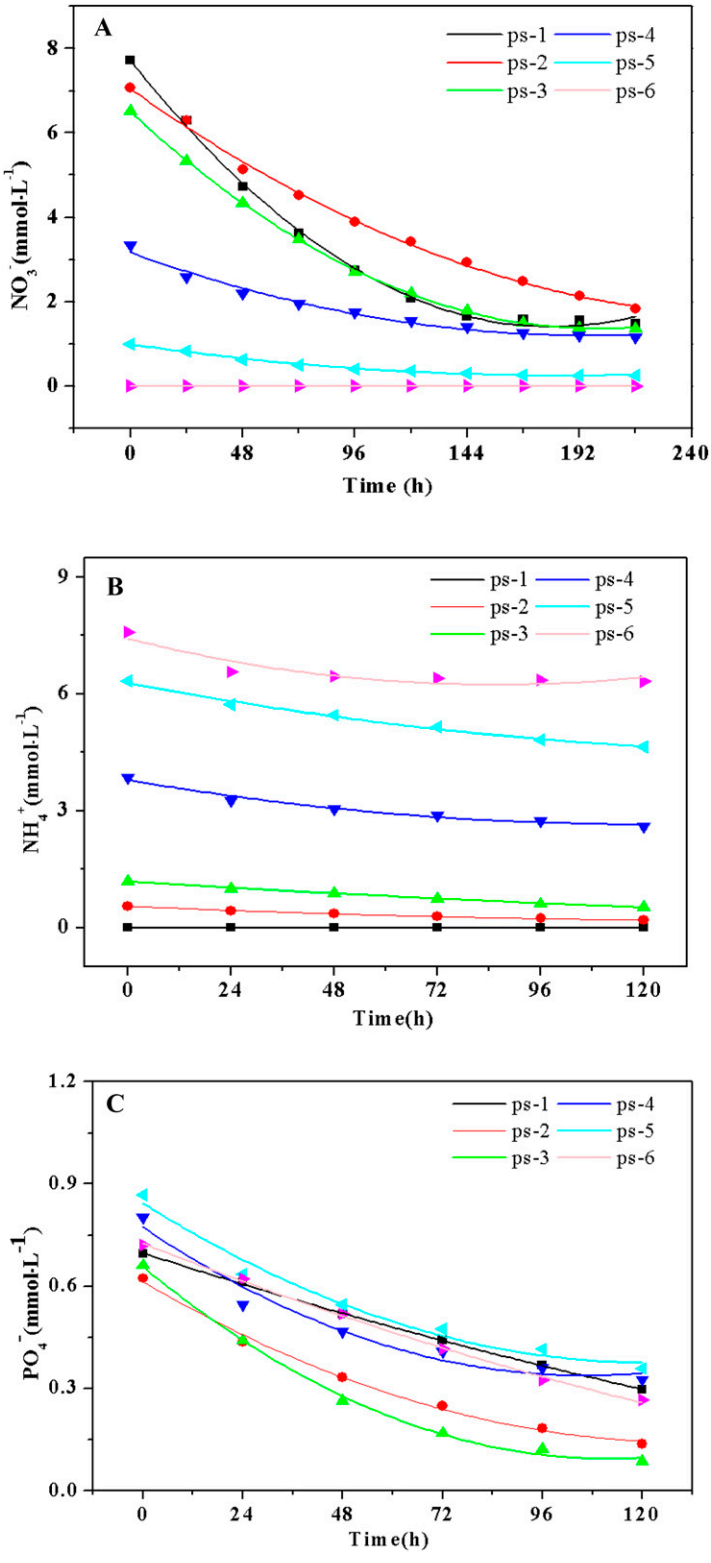

Fig. 5. Fitting curves of the relationship between concentrations of NH_4^+, NO_3^-, and PO_4^- and the absorption time in *I. pseudacorus.* (**A**) Fitting curves of the relationship between the concentrations of NH_4^+ and the absorption time in *I. pseudacorus*. (**B**) Fitting curves of the relationship between the concentrations of NO_3^- and the absorption time in *I. pseudacorus*. (**C**) Fitting curves of the relationship between the concentrations of PO_4^- and the absorption time in *I. pseudacorus.*

2004). The cellular metabolic energy stored in *I. pseudacorus* at the ps-4 level had reduced. Second, nitrate nitrogen would promote photosynthetic carbon assimilation enzymes and chlorophyll synthesis in *I. pseudacorus* and *I. japonica* (Fig. 6). Researchers have reported that amount of nitrate nitrogen during the cultivation of *Hemarthria altissima* was beneficial for the photosynthetic carbon assimilation and chlorophyll synthesis, further the improvement of photosynthesis ability and the promotion of its growth and development (Guo et al., 2007; Wei et al., 2020). The net photosynthetic rates of *I. pseudacorus* at the ps-3 level were significantly higher than those at the ps-4 level (Fig. 6), which indicated that the solar energy captured by *I. pseudacorus* at the ps-3 level was greater than that at the ps-4 level. The results showed that amount of nitrate was beneficial to plant growth of *I. pseudacorus* and *I. japonica* (Table 2). Researchers have reported that high concentration of ammonium has an apparent toxic effect on the photosynthetic rates in plants (Cumming and Weinstein, 1990). A high concentration of ammonium could decrease the P_N of *I. japonica* at ja-5 and ja-6 levels and those at ja-5 and ja-6 levels. Studies have shown that excessive application of NH_4^+ inhibited the absorption of potassium (K^+) and calcium ions (Ca^{2+}) in plants, resulting in various metabolic disorders and ammonia poisoning in plants (Jampeetong et al., 2012; Li et al., 2006; Wang and Luo, 2009).

A low value of K_m and a high value of V_{max} indicate a high removal efficiency of ions from wastewater (Zhu et al., 2020). The values of V_{max} for NO_3^-, NH_4^+, and PO_4^- uptake in *I. pseudacorus* were higher than those in *I. japonica* at each treatment level (Tables 3 and 4). The results shown that removal of nitrogen and phosphorus for *I. pseudacorus* higher than *I. japonica*. Studies have shown that HATS for NO_3^- will be activated when the value of K_m is lower than 1 mmol·L^{-1}, whereas LATS will be activated when the value of K_m is higher than 1 mmol·L^{-1} (Krapp et al., 2014). The high-affinity NO_3^- uptake system would be activated in ps-5 and ja-5 (Tables 3 and 4). The results reflected that NO_3^- was transported through LATS at the other levels. It is dominated by HATS when the concentration of NH_4^+ is lower than 1 mmol·L^{-1} (Kronzucker et al., 1996). However, the LATS will become dominant when the concentration of NH_4^+ is ≥1 mmol·L^{-1} (Kronzucker et al., 1996). The results shown that the high-affinity NH_4^+ uptake system was activated in the intracellular membranes at ps-2, ps-3, ja-2, and ja-3 levels (Tables 3 and 4), but NH_4^+ was transported through the LATS at ps-4, ps-5, ps-6, ja-4, ja-5, and ja-6 levels. When suffering from phosphorus deficiency, plants absorb phosphorus through HATS, and the unit of K_m is always μmol·L^{-1} (Mei et al., 2012). LATS prevails in plants, and the unit of K_m is mmol·L^{-1} (Muchhal et al., 1996; Nielsen and Barber, 1978). The PO_4^- was transported through the HATS at ps-6 and ja-1 levels (Tables 3 and 4). The low-affinity PO_4^- uptake system was activated at other levels.

The absorption and assimilation of phosphate are influenced by inorganic nitrogen in plants (Guo et al., 2006). First, the degree of polarization and structure of the cell membrane are changed by inorganic nitrogen resources (Ai et al., 2009; Zhou et al., 1998). Second, the proteins of phosphate transporters located on the cell membrane are closely

Table 3. Kinetic parameters for NH_4^+, NO_3^-, and PO_4^- uptake in *I. pseudacorus*.

	NO_3^-			NH_4^+			PO_4^-		
Number	V_{max}	K_m	R^2	V_{max}	K_m	R^2	V_{max}	K_m	R^2
ps-1	70.37 ± 0.13 a	3.31 ± 0.10 a	0.98	0.00	0.00	0.00	3.87 ± 0.03 c	0.45 ± 0.02 a	0.99
ps-2	60.50 ± 0.14 b	2.91 ± 0.12 a	0.99	4.97 ± 0.22 e	0.25 ± 0.01 d	0.99	6.33 ± 0.77 b	0.48 ± 0.03 a	0.99
ps-3	50.80 ± 1.20 c	1.64 ± 0.18 b	0.99	7.07 ± 0.03 d	0.42 ± 0.01 d	0.97	8.07 ± 0.09 a	0.19 ± 0.01 b	0.99
ps-4	21.37 ± 2.63 d	1.65 ± 0.04 b	0.98	19.77 ± 0.38 c	2.81 ± 0.06 c	0.98	8.07 ± 0.09 a	0.48 ± 0.03 a	0.98
ps-5	8.90 ± 0.40 e	0.55 ± 0.11 c	0.99	21.13 ± 0.18 b	4.93 ± 0.01 b	0.97	7.93 ± 0.12 a	0.45 ± 0.02 a	0.99
ps-6	0.00	0.00	0.00	26.96 ± 0.48 a	6.52 ± 0.18 a	0.93	4.53 ± 0.22 c	0.28 ± 0.06 b	0.98

The mean ± SE is followed by different lowercase letters in the same column when values differ significantly at $P \leq 0.05$ according to one-way ANOVA. The unit of V_{max} is $\mu mol \cdot L^{-1} \cdot h^{-1}$, and the unit of K_m is $mmol \cdot L^{-1} \cdot h^{-1}$, the same below. ps = the growth indices of *I. pseudacorus*.

Table 4. Kinetic parameters for NH_4^+, NO_3^-, and PO_4^- uptake in *I. japonica*.

	NO_3^-			NH_4^+			PO_4^-		
Number	V_{max}	K_m	R^2	V_{max}	K_m	R^2	V_{max}	K_m	R^2
ja-1	28.77 ± 0.70 a	8.29 ± 0.03 a	0.99	0.00	0.00	0.00	1.83 ± 0.28 d	0.48 ± 0.04 d	0.99
ja-2	25.70 ± 0.15 b	7.82 ± 0.02 b	0.99	4.67 ± 0.06 d	0.71 ± 0.00 e	0.99	2.27 ± 0.03 bc	0.56 ± 0.00 c	0.99
ja-3	24.67 ± 0.15 b	6.79 ± 0.01 c	0.99	8.60 ± 0.05 c	0.97 ± 0.01 d	0.94	3.57 ± 0.03 a	0.55 ± 0.00 c	0.99
ja-4	23.37 ± 0.17 c	2.74 ± 0.01 d	0.97	14.63 ± 0.08 b	3.94 ± 0.01 c	0.98	2.07 ± 0.03 cd	0.56 ± 0.01 c	0.99
ja-5	5.53 ± 0.03 d	0.57 ± 0.00 e	0.96	12.40 ± 0.36 b	6.65 ± 0.09 b	0.99	2.67 ± 0.04 b	0.63 ± 0.00 b	0.99
ja-6	0.00	0.00	0.00	18.37 ± 0.41 a	7.27 ± 0.11 a	0.99	2.63 ± 0.02 b	0.71 ± 0.01 a	0.94

The mean ± SE is followed by different lowercase letters in the same column when values differ significantly at $P \leq 0.05$ according to one-way ANOVA. ja = the growth indices of *I. japonica*.

Table 5. Correlation analysis of the cell metabolic energy and kinetic parameters for NH_4^+, NO_3^-, and PO_4^- uptake in *I. pseudocorus.*

	PO_4^--V_{max}	PO_4^--K_m	NH_4^+-V_{max}	NH_4^+-K_m	NO_3^--V_{max}	NO_3^--K_m
ps-G_B[z]	−0.034	0.483**	0.879**	0.850**	−0.872**	−0.918**
PO_4^--V_{max}		0.517*	0.172	0.013	−0.194	−0.147
PO_4^--K_m			0.807**	0.685**	−0.804**	−0.628**
NH_4^+-V_{max}				0.936**	−0.995**	−0.936**
NH_4^+-K_m					−0.944**	−0.924**
NO_3^--V_{max}						0.946**

[z]ps-G_B is the cellular metabolic energy of *I. pseudacorus* after the 10th day of treatment although different nitrogen sources.
*, **Significant correlation at the 0.05 or 0.01 levels, respectively.

Table 6. Correlation analysis of the cell metabolic energy and kinetic parameters for NH_4^+, NO_3^-, and PO_4^- uptake in *I. japonica.*

	PO_4^--V_{max}	PO_4^--K_m	NH_4^+-V_{max}	NH_4^+-K_m	NO_3^--V_{max}	NO_3^--K_m
ja-G_B[z]	0.188	0.800**	0.918**	0.904**	−0.822**	−0.917**
PO_4^--V_{max}		0.188	0.274	0.111	−0.234	−0.114
PO_4^--K_m			0.815**	0.853**	−0.884**	−0.816**
NH_4^+-V_{max}				0.880**	−0.770**	−0.908*
NH_4^+-K_m					−0.943**	−0.911**
NO_3^--V_{max}						0.900**

[z]ja-G_B is the cellular metabolic energy of *I. japonica* after the 10th day of treatment although different nitrogen source.
*, **Significant correlation at the 0.05 or 0.01 levels, respectively.

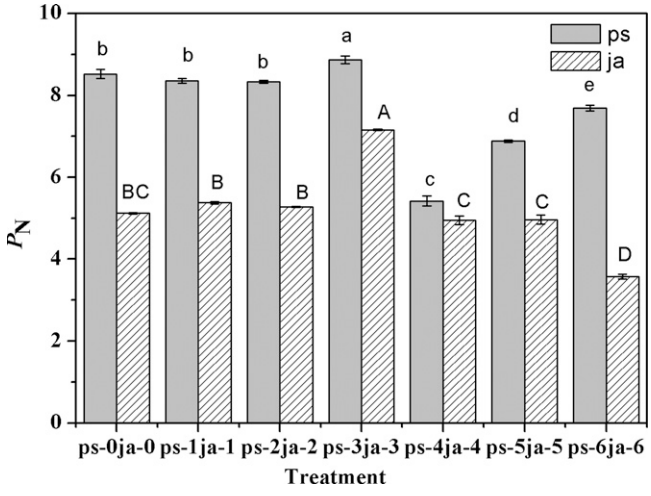

Fig. 6. Effects of different nitrogen sources on the net photosynthetic rate (P_N) of *I. japonica* and *I. pseudacorus*. a, b, c, d, and e = the mean ± SD and significant differences at the 5% level of *I. pseudacorus*. A, B, C, and D = the mean ± SD and significant differences at the 5% level of *I. japonica*.

related to the nitrogen inside and outside the plant cells (Versaw and Garcia, 2017; Xu et al., 2018). The active transport of nitrogen dominated by the binding proteins is equal to the absorption of nitrogen by plants (Versaw and Garcia, 2017; Xu et al., 2018).

Studies have shown that the NO_3^- or NH_4^+ could have similar affinity and absorption rate, and the most suitable environment for plant could not be distinguished when the concentration of ammonium or nitrate have no significant difference between treatments (Wang et al., 2016). In conclusion, high concentration of ammonia (ps-4, ps-5, ps-6 and ja-4, ja-5, ja-6) was not conducive to *I. pseudacorus* and *I. japonica*. When there was no significant difference in the concentration of ammonium or nitrate between treatments, the higher value of cellular metabolic energy indicated the better status of plant growth.

The results showed that the NO_3^-:NH_4^+ = 27:3 treatment level was more suitable for *I. pseudacorus* and *I. japonica* compared with other treatment levels.

Conclusion

Overall, the increase of NH_4^+ concentration could increase the cellular metabolic energy stored in *I. pseudocorus* and *I. japonica* when the concentration of total nitrogen was the same. The results indicate that the cellular metabolic energy stored in *I. pseudacorus* was lower than those in *I. japonica*, which made the removal for NO_3^- and NH_4^+ in *I. pseudacorus* higher than those in *I. japonica*. The cellular metabolic energy stored in *I. pseudacorus* and *I. japonica* could also affect the phosphate and photosynthetic rate. The results showed that the removal for NO_3^-, NH_4^+, and $H_2PO_4^-$ in *I. pseudacorus* were higher than those in *I. japonica* at each treatment level. These results demonstrate that the NO_3^-:NH_4^+ = 27:3 treatment level was more suitable for *I. pseudacorus* and *I. japonica* compared with other treatment levels. This indicates that the higher value of cellular metabolic energy was suitable for plant growth when there was no significant difference in the concentration of ammonium or nitrate between treatments. The results can provide a simple and rapid solution for removal of nitrogen by the determination of cellular metabolic energy.

Literature Cited

Abe, F., R.F. Chen, and T. Yamauchi. 1991. Iridals from *Belamcanda chinensis* and *Iris Japonica*. Phytochemistry 30:3379–3382, https://doi.org/10.1016/0031-9422(91)83213-5.

Ai, P.H., S.B. Sun, J.N. Zhao, X.R. Fan, and W.J. Xin. 2009. Two rice phosphate transporters, OsPht1;2 and OsPht1;6, have different functions and kinetic properties in uptake and translocation. Plant J. Cell Molec. Biol. 57:798–809, https://doi.org/10.1111/j.1365-313X.2008.03726.x.

Anderson, C.W. 1980. Tissue culture propagation red and black Raspberry, *Rubus idaeus* and *R. occidentalis*. Acta Hort. 112:13–20, https://doi.org/10.17660/ActaHortic.1980.112.1.

Aoki, K. 1991. Nernst equation complicated by electric random percolation at conducting polymer-coated electrodes. J. Electroanal. Chem. 310:1–12, https://doi.org/10.1016/0022-0728(91)85247-M.

Chen, G.Y., G.X. Li, and K. Tang. 2013. Kinetics of nitrogen and phosphorus uptake by root system of *Iris pseudacorus* L. and *Typha angustifolia* L. J. Environ. Eng. 12:46–50.

Colmer, T.D. and A.J. Bloom. 1998. A comparison of NH_4^+ and NO_3^- net fluxes along roots of rice and maize. Plant Cell Environ. 21:240–246, https://doi.org/10.1046/j.1365-3040.1998.00261.x.

Cui, J.H., C.Q. Yu, N. Qiao, X.L. Xu, Y.Q. Tian, and O.Y. Hua. 2017. Plant preference for NH_4^+ versus NO_3^- at different growth stages in an alpine agroecosystem. Field Crops Res. 201:192–199, https://doi.org/10.1016/j.fcr.2016.11.009.

Cumming, J.R. and L.H. Weinstein. 1990. Nitrogen source effects on Al toxicity in nonmycorrhizal and mycorrhizal pitch pine (*Pinus rigida*) seedlings. I. Growth and nutrition. Can. J. Bot. 68:2644–2652, https://doi.org/10.1139/b90-334.

Feng, Y., Q.F. Chen, J.Y. Li, B.B. Guo, T. Liu, L. Li, and L. Qi. 2020. Comparison of purification ability of aquatic plants under different concentrations of nitrogen and phosphorus in tailrace of livestock wastewater. J. Agro-Environment Sci. 39:2397–2408, https://doi.org/10.11654/jaes.2020-0816.

Guo, S., Y. Zhou, Q. Shen, and F. Zhang. 2007. Effect of ammonium and nitrate nutrition on some physiological processes in higher plants-growth, photosynthesis, photorespiration, and water relations. Plant Biol. 9:21–29, https://doi.org/10.1055/s-2006-924541.

Guo, Z.H., L.Y. He, and C.G. Xu. 2006. Effects of phosphorus levels on root growth and nitrogen, phosphorus and potassium absorption of low phosphorus tolerant in *Oryza sativa* L. seedlings. Chin. J. Appl. Environ. Biol. 12:449–452, https://doi.org/10.3321/j.issn:1006-687X.2006.04.001.

Hardie, H. and D. Grahame. 2015. AMPK: Positive and negative regulation, and its role in whole-body energy homeostasis. Curr. Opin. Cell Biol. 33:1–7, https://doi.org/10.1016/j.ceb.2014.09.004.

Hu, X.H. 2008. Phosphorus and life activities. Biol. Teach. 33:62–63, https://doi.org/10.3969/j.issn.1004-7549.2008.07.037.

Jampeetong, A., H. Brix, and S. Kantawanichkul. 2012. Effects of inorganic nitrogen forms on growth, morphology, nitrogen uptake capacity and nutrient allocation of four tropical aquatic macrophytes (*Salvinia cucullate, Lpomoea aqnatica, Cyperns involucratus* and *Vetiveria Zizanioides*). Aquat. Bot. 97(1):10–16, https://doi.org/10.1016/j.aquabot.2011.10.004.

Ji, X.M., L. Xu, Y.F. Xie, Z.C. Wang, F.Z. Chen, W.D. Chen, and Z.Y. Luo. 2015. Effects of hydrophytes on removal of nitrogen and phosphorus in different levels of eutrophic water. Southwest China J. Agr. Sci. 02:809–814, https://doi.org/10.16213/j.cnki.scjas.2015.02.068.

Kochian, L.V. and X. Jiao. 1985. Potassium transport in corn roots: IV. characterization of the linear component. Plant Physiol. 79:771–776, https://doi.org/10.1104/pp.79.3.771.

Konnerup, D. and H. Brix. 2010. Nitrogen nutrition of *Canna indica*: Effects of ammonium versus nitrate on growth, biomass allocation, photosynthesis, nitrate reductase activity and N uptake rates. Aquat. Bot. 92(2):142–148, https://doi.org/10.1016/j.aquabot.2009.11.004.

Krapp, A., L.C. David, C. Chardin, T. Girin, A. Marmagne, A. Leprince, S. Chaillou, S. Ferrario-Méry, C. Meyer, F. Daniel-Vedele. 2014. Nitrate transport and signalling in Arabidopsis. J. Expt. Bot. 65:789–798, https://doi.org/10.1093/jxb/eru001.

Kronzucker, H.J., M.Y. Siddiqi, and A. Glass. 1996. Kinetics of NH_4^+ influx in spruce. Plant Physiol. 110:773–779, https://doi.org/10.1104/pp.110.3.773.

Li, C.Y., X.Q. Kong, and H.Z. Dong. 2020. Nitrate uptake, transport and signaling regulation pathways. J. Nuclear Agr. Sci. 34:84–95.

Li, X., Y.F. Han, and J.F. Liu. 2006. Effects of nitrogen forms on growth and enzymes related to nitrogen metabolism of *Phellodendron amurense*. Chinese Bul. Bot. 23(3):255–261, https://doi.org/10.3969/j.issn.1674-3466.2006.03.004.

Liu, T. and Z.L. Shang. 2016. Research progress on molecular regulation of ammonium uptake and transport in plant. Plant Physiol. J. 52:799–809, https://doi.org/10.13592/j.cnki.ppj.2015.0693.

Mark, W., B. Dev, B. Konstantine, and K. Herbert. 2008. Alleviation of rapid, futile ammonium cycling at the plasma membrane by potassium reveals K^+-sensitive and -insensitive components of NH_4^+ transport. J. Expt. Bot. 59:303–313, https://doi.org/10.1093/jxb/erm309.

Mei, J., J.W. Hu, X.F. Huang, L.Y. Fu, J. Luo, and M. Jia. 2012. Release kinetics of phosphorus in sediments from Baihua Lake. Adv. Environ. Engineer. 599:91–95, https://doi.org/10.4028/www.scientific.net/AMR.599.91.

Muchhal, U.S., J.M. Pardo, and K.G. Raghothama. 1996. Phosphate transporters from the higher plant *Arabidopsis thaliana*. Proc. Natl. Acad. Sci. USA 93:10519–10523, https://doi.org/10.1073/pnas.93.19.10519.

Mwesigwa, J., D.J. Collins, and A.G. Volkov. 2000. Electrochemical signaling in green plants: Effects of 2,4-dinitrophenol on variation and action potentials in soybean. Bioelectrochemistry 51(2):201–205, https://doi.org/10.1016/S0302-4598(00)00075-1.

Nielsen, N.E. and S.A. Barber. 1978. Differences among genotypes of corn in the kinetics of P uptake. Agron. J. 70:695–698, https://doi.org/10.2134/agronj1978.00021962007000050001x.

Poothong, S. and B.M. Reed. 2016. Optimizing shoot culture media for *Rubus* germplasm: The effects of NH_4^+, NO_3^-, and total nitrogen. In Vitro Cell. Dev. Biol. Plant 52:265–275, https://doi.org/10.1007/s11627-016-9750-0.

Ramage, C.M. 2002. Inorganic nitrogen requirements during shoot organogenesis in tobacco leaf discs. J. Expt. Bot. 53:1437–1443, https://doi.org/10.1093/jexbot/53.373.1437.

Reuveni, M. 1992. Utilization of metabolic energy under saline conditions: Changes in properties of ATP dependent enzymes in plant cells grown under saline conditions. Biol. Plant. 34:181–191, https://doi.org/10.1007/BF02925865.

Schönleber, M. and E. Ivers-Tiffée. 2015. Approximability of impedance spectra by RC elements and implications for impedance analysis. Electrochem. Commun. 58:15–19, https://doi.org/10.1016/j.elecom.2015.05.018.

Shu, S., X. Duan, Y. Zhao, and H. Xiong. 2016. A model based on time, space, energy and iterative mechanism for woody plant metabolic rates and biomass. J. Biobased Mater. Bioenergy 10:184–194, https://doi.org/10.1166/jbmb.2016.1601.

Siddiqi, M.Y., A.D. Glass, T.J. Ruth, and T.W. Rufty. 1992. Studies of the uptake of nitrate in barley: I. kinetics of $^{13}NO_3^-$ influx. Plant Physiol. 99:456–463, https://doi.org/10.1104/pp.93.4.1426.

Stitt, M. 1999. Nitrate regulation of metabolism and growth. Curr. Opin. Plant Biol. 2:178–186, https://doi.org/10.1016/S1369-5266(99)80033-8.

Sun, S.P., D.R. Xing, L. Zhang, Y.N. Ai, X.H. Fun, and Q.J. Zhang. 2007. Determination of Nitrate-N in water by 2-Isopropyl-5-methyphenol spectrophotometry. J. Environ. Health 4:256–258, https://doi.org/10.3969/j.issn.1001-5914.2007.04.027.

Tan, G. and L. Mao. 1998. Discuss of problem about Nash reagent photometry to determine ammonia and nitrogen in sewage. Environ. Protection Oil Gas Fields. 04:15–17, https://doi.org/CNKI:SUN:YQTB.0.1998-04-003.

Tho, B.T., C. Lambertini, F. Eller, H. Brix, and B.K. Sorrell. 2017. Ammonium and nitrate are both suitable inorganic nitrogen forms for the highly productive wetland grass *Arundo donax*, a candidate species for wetland paludiculture. Ecol. Eng. 105:379–386, https://doi.org/10.1016/j.ecoleng.2017.04.054.

Vanhercke, T., E. Tachy, Q. Liu, X.R. Zhou, P. Shrestha, U.K. Divi, J.-P. Ral, M.P. Mansour, P.D. Nichols, C.N. James, P.J. Horn, K.D. Chapman, F. Beaudoin, N. Ruiz-López, P.J. Larkin, R.C. de Feyter, S.P. Singh, and J.R. Petrie. 2014. Metabolic engineering of biomass for high

energy density: Oilseed-like triacylglycerol yields from plant leaves. Plant Biotechnol. J. 12:231–239, https://doi.org/10.1111/pbi.12131.
Versaw, W.K. and L.R. Garcia. 2017. Intracellular transport and compartmentation of phosphate in plants. Curr. Opin. Plant Biol. 39:25–30, https://doi.org/10.1016/j.pbi.2017.04.015.
Wang, K.C. and Q.Y. Luo. 2009. Effects of NH_4^+/NO_3^- ratio in applied supplementary fertilizer on nitrogen metabolism, photosynthesis and growth of *Isatis indigotica.* Chinese J. Chinese Materia Medica 34(16):2039–2042, https://doi.org/10.3321/j.issn:1001-5302.2009.16.008.
Wang, M.Y., M.Y. Siddiqi, T.J. Ruth, and A. Glass. 1994. Ammonium uptake by rice roots. Plant Physiol. 104:899–906, https://doi.org/10.1104/pp.104.3.899.
Wang, B., F.X. Wen, and B. Xiao. 2016. Effects of nitrate in water on the growth of *Iris pseudacorus* L. and its adsorption capacity of nitrogen in a simulated experiment. Chinese J. Environ. Sci. 9:3447–3452, https://doi.org/10.13227/j.hjkx.2016.09.024.
Wang, X.D., Z.W. Yu, Y. Shi, and X.Y. Wang. 2006. Effects of phosphorus on activities of enzymes related to nitrogen metabolism in flag leaves and protein contents in grains of wheat. Acta Agronomica Sinica 32(3): 339–344, https://doi.org/10.3321/j.issn:0496-3490.2006.03.004.
Wang, X.L. and X.F. Lu. 2020. Research progress on mechanism of nitrogen metabolism involved in plant stress resistance. Guihaia 40:583–591, https://doi.org/10.11931/guihaia.gxzw201901007.
Wang, Z., Q. Song, L. Shuai, R. Hun, and F. Zhou. 2020. Metabolic and proteomic analysis of nitrogen metabolism mechanisms involved in the sugarcane-*Fusarium verticillioides* interaction. J. Plant Physiol. 4:251, https://doi.org/10.1016/j.jplph.2020.153207.
Wei, H.D. 2003. Rapid determination of available P_2O_5 in DAP by phosphomolybdovanadate spectrophotometric method. Phosphorus Compound Fert. 03:60–61, https://doi.org/10.3969/j.issn.1007-6220.2003.03.023.
Wei, X.W., Y. Tan, L. Guo, F.Y. Liu, F. Liu, and H.W. Xu. 2020. Effects of nitrogen forms on photosynthetic carbon assimilation enzymes and chlorophyll synthesis in *Hemarthria altissima.* Jilin Normal Univ. J. 41(3):106–111, https://doi.org/10.16862/j.cnki.issn1674-3873.2020.03.017.
Xu, Z., W.X. Wang, L. Xu, and K.K. Yi. 2018. Research progress in molecular mechanism of rice phosphorus uptake and translocation. J. Plant Nutr. Fert. 24:1378–1385, https://doi.org/10.11674/zwyf.18052.
Xu, Z.Z. and G.S. Zhou. 2004. Research advance in nitrogen metabolism of plant and its environmental regulation. J. Appl. Ecol. 15(3):511–516.
Yang, H.Y., Y.G. Wang, H.L. Li, X. Wang, F. Xu, and S.S. Li. 2017. Absorption capacity of two kinds of floating bed plants for nitrogen and phosphorus removal in waterbody and the purification effect on water quality. Water Purification Technol. 36(3):63–67, https://doi.org/10.15890/j.cnki.jsjs.2017.03.010.
Yuan, H.Z., Y.X. Zhang, Q.Q. Liu, Y.H. Yang, J. Miao, and S.Z. Huang. 2018. Study on purification of some species of *Iris* L. for different eutrophic water in different seasons. Southwest China J. Agr. Sci. 31(1):165–170, https://doi.org/10.16213/j.cnki.scjas.2018.1.029.
Zhou, J.J., F.L. Theodoulou, I. Muldin, B. Ingemarsson, and A.J. Miller. 1998. Cloning and functional characterization of a *Brassica napus* transporter that is able to transport nitrate and histidine. J. Biol. Chem. 273:12017–12023, https://doi.org/10.1074/jbc.273.20.12017.
Zhu, L.W., C.M. Zhou, C.H. Bai, Y.C. Qu, and L.X. Yao. 2020. Kinetics of nitrogen and phosphorus uptake by litchi under different temperatures and nitrogen forms. J. Plant Nutr. Fert. 26:869–887, https://doi.org/10.11674/zwyf.19325.

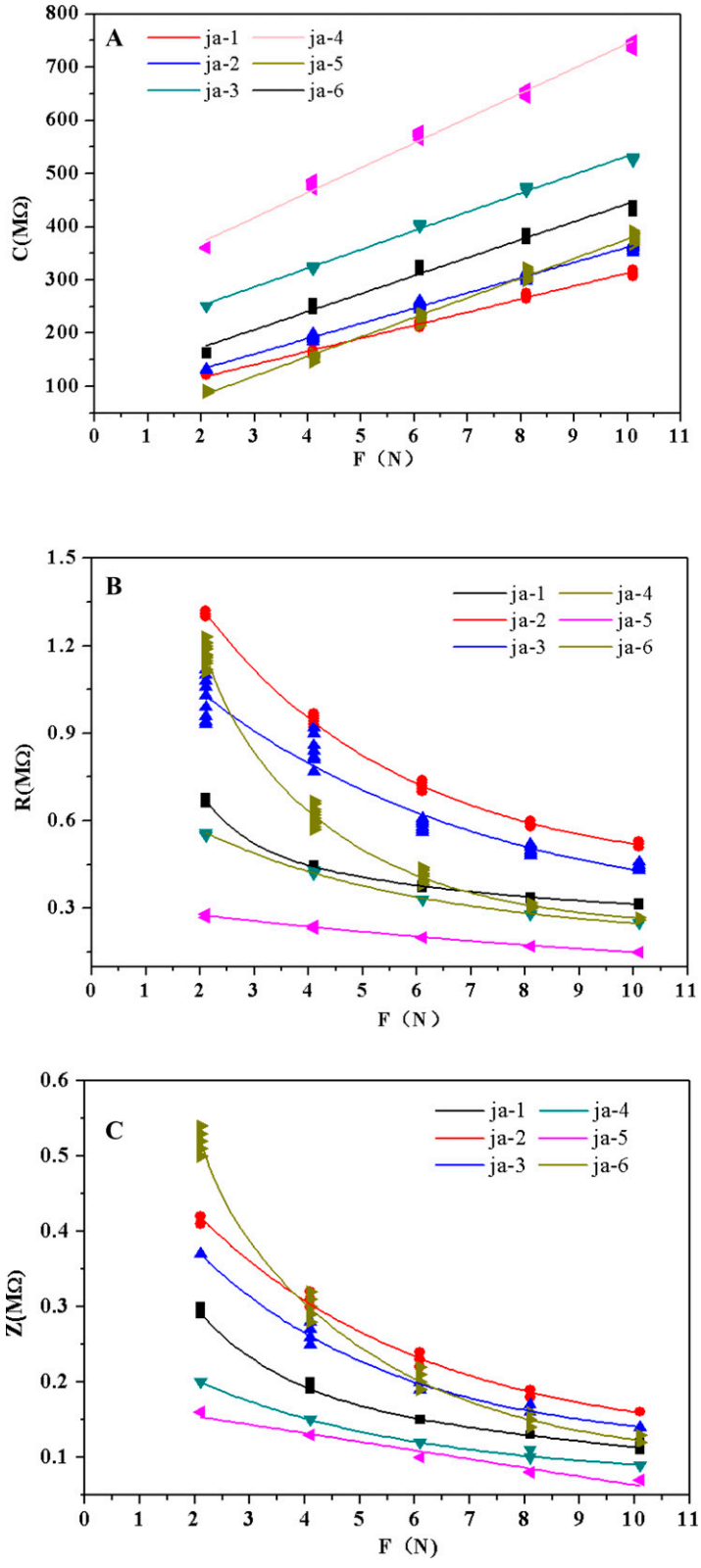

Supplemental Fig. 1. Fitting curves of the relationships among capacitance (C), resistance (R), impedance (Z), and gripping force (F) of *I. japonica* under different inorganic nitrogen sources. (**A**) The relationship between the physiological C and F of *I. japonica*. (**B**) The relationship between the physiological R and F of *I. japonica*. (**C**) The relationship between the physiological Z and F of *I. japonica*.